

Retraction

Retracted: Driving Detection Based on the Multifeature Fusion

Journal of Control Science and Engineering

Received 15 August 2023; Accepted 15 August 2023; Published 16 August 2023

Copyright © 2023 Journal of Control Science and Engineering. This is an open access article distributed under the Creative Commons Attribution License, which permits unrestricted use, distribution, and reproduction in any medium, provided the original work is properly cited.

This article has been retracted by Hindawi following an investigation undertaken by the publisher [1]. This investigation has uncovered evidence of one or more of the following indicators of systematic manipulation of the publication process:

- (1) Discrepancies in scope
- (2) Discrepancies in the description of the research reported
- (3) Discrepancies between the availability of data and the research described
- (4) Inappropriate citations
- (5) Incoherent, meaningless and/or irrelevant content included in the article
- (6) Peer-review manipulation

The presence of these indicators undermines our confidence in the integrity of the article's content and we cannot, therefore, vouch for its reliability. Please note that this notice is intended solely to alert readers that the content of this article is unreliable. We have not investigated whether authors were aware of or involved in the systematic manipulation of the publication process.

Wiley and Hindawi regrets that the usual quality checks did not identify these issues before publication and have since put additional measures in place to safeguard research integrity.

We wish to credit our own Research Integrity and Research Publishing teams and anonymous and named external researchers and research integrity experts for contributing to this investigation.

The corresponding author, as the representative of all authors, has been given the opportunity to register their agreement or disagreement to this retraction. We have kept a record of any response received.

References

- [1] Q. Yang and Y. Lu, "Driving Detection Based on the Multifeature Fusion," *Journal of Control Science and Engineering*, vol. 2022, Article ID 8266295, 7 pages, 2022.

Research Article

Driving Detection Based on the Multifeature Fusion

Qiufen Yang  and Yan Lu 

Information Department, Hunan Open University, Changsha, Hunan 410001, China

Correspondence should be addressed to Qiufen Yang; 1332304234@post.usts.edu.cn

Received 23 May 2022; Revised 6 June 2022; Accepted 10 June 2022; Published 30 June 2022

Academic Editor: Jackrit Suthakorn

Copyright © 2022 Qiufen Yang and Yan Lu. This is an open access article distributed under the Creative Commons Attribution License, which permits unrestricted use, distribution, and reproduction in any medium, provided the original work is properly cited.

In order to solve the problems of facial feature localization and driver fatigue state identification methods in driving fatigue detection, a driving detection method based on the multifeature fusion was proposed. This method uses a supervised descent algorithm to simultaneously locate multiple facial features of drivers. On the basis of blink, yawn and nod judgment, multiple characteristic values of blink frequency, yawn frequency, and nod frequency of drivers were extracted to establish a fatigue detection sample database, and a naive Bayes classifier was constructed to judge fatigue. When the driver appears fatigue driving, warning information is given in time in order to prevent traffic accidents. The experimental results show that two sample videos were selected for testing. The accuracy rate of video sample 1 and video sample 2 was 94.74% and 95.00%, respectively. *Conclusion.* In the actual driving environment video test results, the discriminant average accuracy of a driver fatigue state reaches 94.87%, which has a good performance.

1. Introduction

According to the official website of the National Bureau of Statistics, by the end of 2019, the number of civil cars in China reached 253.7638 million, with a year-on-year growth of 9.23%. The number of car drivers reached 39,7528,600, with a year-on-year increase of 7.66% [1]. Cars greatly facilitate people's travel. In transportation, its role is irreplaceable, but the popularity of cars also inevitably has caused the frequent occurrence of road traffic accidents. China is one of the countries with the largest number of road traffic accidents in the world, which not only leads to a huge number of casualties, brings irreversible losses to individuals, families, and the country, but also seriously hinders the development of China's economy and social stability. As can be seen from the data of automobile traffic accidents in China in recent 10 years [2] shown in Figure 1 below, since 2010, the number of accidents and the number of injuries have basically changed simultaneously, and the number of deaths fluctuates slightly. However, it is still not optimistic, the direct loss of property due to accidents is huge, and the overall trend is on the rise.

Fatigue driving is one of the main causes of traffic accidents, and the number of traffic accidents caused by it is

increasing year by year [3]. Fatigue driving has a strong concealability, and usually only the driver himself can detect it. Therefore, if the driver can be timely and accurately detected and given some warning after determining the fatigue state of the driver, the injury of fatigue driving can be greatly reduced. Therefore, as an important means to reduce traffic accidents, fatigue driving detection and early warning have gradually become an important technical research hotspot in the academic field and the automobile industry at home and abroad.

2. Literature Review

By obtaining the maximum zero speed percentage and the maximum angle standard deviation in the steering wheel rotation process, Nemcova et al. identified the fatigue degree of the driver through the classifier and established the fatigue detection method of the highway under the condition of constant lane change [4]. Bakker et al. studied steering wheel angle and the steering wheel angle rate. Using these two parameters to establish the coordinate system, it is found that when the driver is awake, the sample points obtained are mostly distributed in an ellipse centered on the origin, while

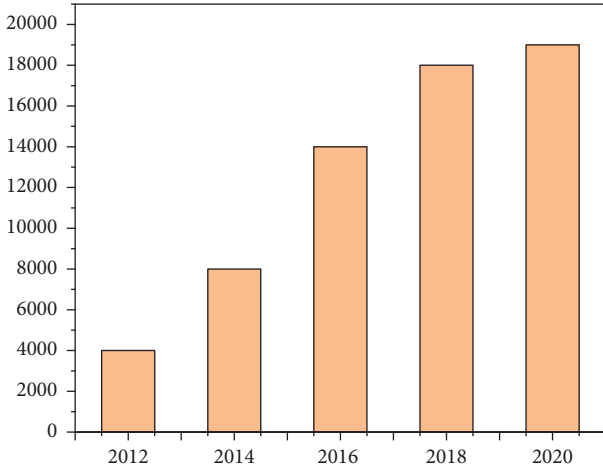


FIGURE 1: Statistical chart of automobile traffic accidents in China from 2010 to 2019.

when the driver is fatigued, the sample points are located far away from the origin [5]. The fatigue degree was judged by heart rate variability (HRV) by Nowara et al. which refers to the time difference between two heartbeats and the change of the ratio of high and low heartbeats with the fatigue degree [6]. Gonzalez et al. used infrared illumination to produce the bright pupil effect for eye detection. First, a bright pupil image under 850 nm infrared light was taken, and then a dark pupil image under 950 nm infrared light was taken. The position and size of the pupil can be obtained by differential processing of two frames of images. The degree of eye-opening is judged according to the size of the pupil, and the driver's fatigue degree is judged by using PERCLOS characteristic parameters [7]. Gomez designed a structure with the camera as the center and two circles of LED around it. For odd frames, the inner LED is lit to form coaxial light, while for even frames, the outer LED is lit to form off-axis light. Coaxial light has a strong ability to reflect into the camera through the eye, while off-axis light has a poor ability to reflect into the camera through the eye, resulting in a bright pupil reaction of one bright pupil position and one dark pupil position in two adjacent images. The position and size of the pupil can be obtained through image difference [8]. Guo used edge detection and Hough circle transformed to locate the features of the driver's mouth for early warning. This method has many constraints and cannot adapt to the randomness and complexity of the driving environment. Therefore, the detection and fusion of multiple facial features has become an inevitable development trend, but in the driving process, the dynamic changes of drivers' head posture, external environment, illumination, and other factors are still difficult to achieve the positioning of multiple features [9].

To solve the above problems, a multifeature fusion algorithm for driver fatigue detection based on machine vision is proposed. A scale invariant feature transform (SIFT) feature value was optimized by the supervised descent

method to achieve facial feature localization. The naive Bayes classifier was combined with blink frequency, yawn frequency, and nod frequency for fatigue judgment. Warning messages are given to drivers when they are tired to prevent traffic accidents. (See Figure 2).

3. The Research Methods

3.1. Facial Feature Localization Algorithm. An active shape model mainly studies the contour of the target object, such as face, hands, heart, lungs, and other objects with little change in the individual shape. The building of active shape model is divided into two parts: training and image matching. The first part is the training part of the model, which needs to find enough target object images as training samples, predetermine the number and position of the required feature points, manually mark the target feature points on each training sample, and obtain its target vector. Then, the target vector set obtained from the training sample is statistically analyzed, normalized by the principal component analysis method, and the average shape vector of the training set is obtained as the initial shape, and the change direction of each point in the shape vector is limited. After the training, the target image is matched for the matching part of the image. The trained initial shape is overlapped with the target image by scaling, rotation, and translation, and the position of each point is optimized and adjusted according to the local grayscale model. The optimal position of each point is searched by the iterative method and finally converges to the shape vector corresponding to the target shape. The specific calculation process of the active shape model [10] is shown in Figure 3.

Human face is a kind of unstructured object with complex detail changes, which makes the traditional detection methods based on the facial skin color and shape characteristics cannot be well adapted to the changes of complex environment [11]. Among numerous research algorithms, the positioning algorithm represented by machine learning is based on a large number of data samples, and the internal relationship of the data is mined through certain learning methods, so that the learning model can still show good learning and reasoning ability in the face of complex environmental changes. Therefore, facial feature localization is considered from the perspective of machine learning. SIFT feature values of facial feature points were optimized by the supervised descent algorithm to build a prediction model of facial feature points. The algorithm model is shown in the following formula [12]:

$$f(x_0 + \Delta x) = \|h(d(x_0 + \Delta x)) - \phi\|_2^2, \quad (1)$$

where, $d(x)$ is the index value of marked feature points, 68 feature points are selected to mark facial feature positions, and $d(x) \in R^{68 \times 1}$ ($R^{68 \times 1}$ is the index matrix of feature points). $h(x)$ is nonlinear feature extraction function, representing SIFT feature values of facial feature points. For the 128-dimensional SIFT feature, $h(d(x)) \in R^{128 \times 68}$. In the training, x_* is the known labeled feature points in the sample

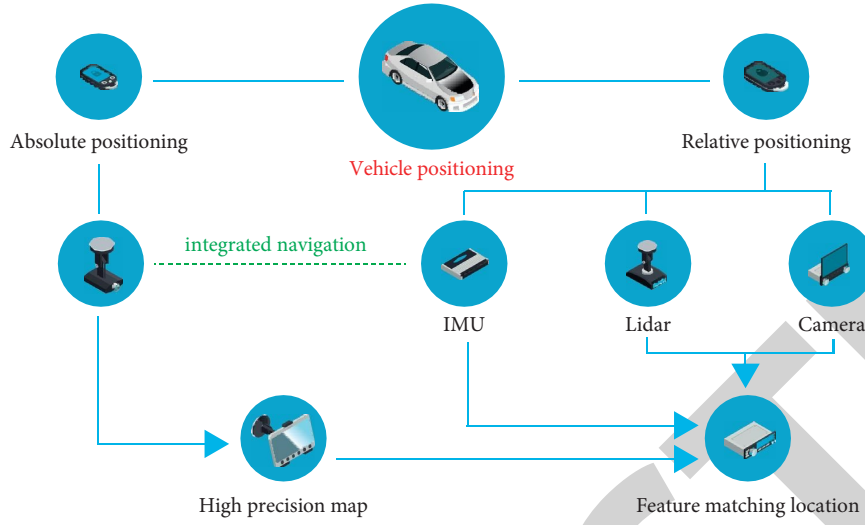


FIGURE 2: Driving detection with a multifeature fusion.

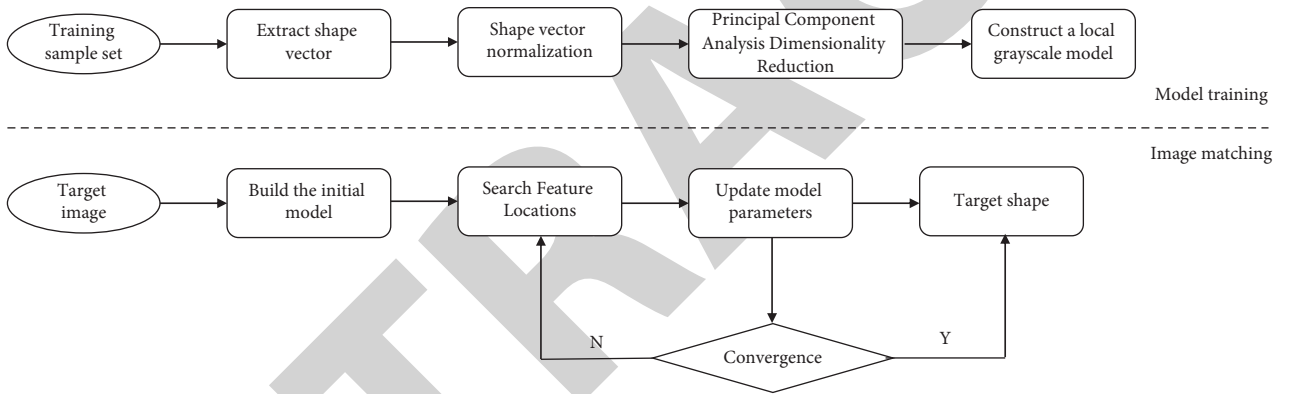


FIGURE 3: Calculation flow of the active shape model.

database, $\phi_* = h(d(x_*))$ is the eigenvalue of labeled feature points, $\phi_* \in R^{128 \times 68}$; x_0 is the initialization feature point.

The model can be regarded as minimizing equation (1) by finding the gradient direction Δx of the feature point. In the process of model training, for the general Newton iteration method, the initial convergence of the feature point x_0 to the marked feature point x_* is only required by obtaining a series of gradient descent directions and updating the scaling coefficient $\Delta x_{k+1} = x_k + \Delta x_k$. Assuming the second derivative of feature extraction function $h(x)$, equation (1) is expanded by the second order Taylor formula to obtain the following equation [13]:

$$f(x_0 + \Delta x) \approx f(x_0) + J_f(x_0)^T \Delta x + \frac{1}{2} \Delta x^T H(x_0) \Delta x, \quad (2)$$

where $J_f(x_0)$, $H(x_0)$ are the Hessian and Jacobian matrices of the model at the initial facial feature points. Formula (3) can be obtained by taking the derivative of $f(x_0 + \Delta x) = 0$ against Δx in formula (2).

$$\Delta x = -H^{-1} J_f = -2H^{-1} J_f^T (\phi_0 - \phi_*), \quad (3)$$

where $J_f = 2J_f^T (\phi_0 - \phi_*)$: let $R_0 = -2H^{-1} J_f^T$, then $\Delta x = R_0 (\phi_0 - \phi_*)$. In this process, the calculation of R_0 will inevitably involve the calculation of Hessian and Jacobian matrices, which will lead to the increase of computational complexity and the existence of strong constraints. Therefore, the supervised descent algorithm is adopted to learn R_0 directly through the training data set, as shown in the following equation:

$$\Delta x = R_0 \phi_0 + b_0, \quad (4)$$

where b_0 is the offset term, and the training process is as follows:

- (1) A set of training set picture $\{d^i\}$ and corresponding labeled feature point set $\{x_*^i\}$ were given, the average facial feature point shape was calculated by normalizing the training sample [14, 15].

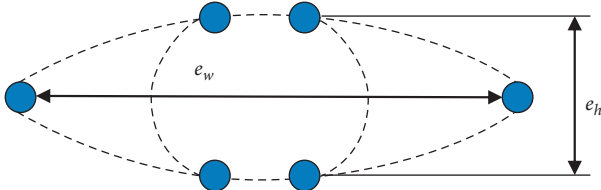


FIGURE 4: Diagram of the eye height-to-width ratio.

- (2) A face detection classifier was used to locate the faces of the training samples, and the average facial feature point shape was used to initialize the facial feature point $\{x_0^i\}$.

- (3) The first descent direction R_0 and deviation term b_0 were calculated, as shown in the following formula:

$$\arg \min_{R_0, b_0} \sum_{d^i} \sum_{x_0^i} \|\Delta x_*^i - R_0 \phi_0^i - b_0\|^2, \quad (5)$$

$x_*^i = x_0^i - x_0^i$, $\phi_0^i = h(d^i(x_0^i))$ is the eigenvalue of the initial facial feature point of the image of the i th training sample.

- (4) The feature point x_i is updated for the first time, as shown in the following equation:

$$x_1 = x_0 + R_0 \phi_0 + b_0. \quad (6)$$

- (5) Steps (3) to (4) are repeated until equation (1) converges.

In model training, $k-1$ descent direction R_{k-1} and deviation b_{k-1} are calculated as shown in equation (7). The k update calculation of feature point x_i is shown in equation (8).

$$\arg \min_{R_k, b_k} \sum_{d^i} \sum_{x_k^i} \|\Delta x_*^{(k-1)i} - R_{k-1} \phi_{k-1}^i - b_{k-1}\|^2, \quad (7)$$

$$x_k = x_{k-1} + R_{k-1} \phi_{k-1} + b_{k-1}. \quad (8)$$

LFPW database was used for model training [16].

3.2. Extraction of Fatigue Eigenvalues. Numerous studies have shown that yawning, frequent nods, and increased blinking occur when the body is tired. Therefore, on the basis of facial feature localization, blink frequency, yawn frequency, and nod frequency were selected as fatigue characteristic values. Firstly, the state judgment of blinking, yawning, and nodding was analyzed [17], taking blinking judgment as an example, as shown in Figure 4.

The eye aspect ratio (e_h/e_w) was selected as the condition for blinking judgment. When $(e_h/e_w) \leq e_t$, it was closed, otherwise, it was open, where, e_t is the judgment threshold of open and close eyes. Yawning is similar to blinking. Head pose estimation. A head pose model was established to predict the head pose p_k by using the supervised descent algorithm based on the head pose described in the literature. Similar to blinking judgment, when $p_k \geq n_t$ is the nodding

state, otherwise, it is the normal state (n_t is the threshold of nodding judgment) [18].

3.3. Design of a Simple Bayesian Classifier. Classification is an important research content in machine learning, pattern recognition, artificial intelligence, and other fields. Many problems in real life can be essentially classified, such as risk prediction, medical diagnosis, spam, fraud detection, and so on. Classification requires learning to produce an objective function (called a classifier or a classification model) that assigns a sample described by an attribute set to a class tag. A classification problem is a two-stage process [19], including the learning stage and the classification stage. In the first stage, the classification algorithm constructs the classification model by analyzing the learning and training data set. The training set consists of tuple data and class tags are associated with it. In the second stage, the classification model constructed by learning is used to classify and predict the sample set with an unknown class label. In general, it is necessary to evaluate the performance of the classifier before using the model for classification. Only the classifier whose performance evaluation indexes meet the specified requirements can be used to classify unknown sample sets.

Due to the excessive optimization effect of the learning algorithm on the training set, the classification model derived from the training set may not be the best, which may mistakenly lead to overoptimistic values of some indexes used to evaluate the model, and researchers are eager to obtain the model with the best classification performance. Therefore, it is very important to compare the performance of different classifiers applied in the same field by calculating evaluation criteria on the test set.

The naive Bayes classifier is based on Bayesian theory, which assumes that conditions are independent among variables and classifies samples by obtaining a posterior probability that they belong to a certain category [20]. The judgment of driving fatigue is regarded as a dichotomous problem. Given sample characteristics, $x = (x_1, x_2, x_3)$, x_1 are blink frequency, x_2 are yawn frequency, and x_3 are nod frequency. The posterior probability distribution of samples is calculated, and the class with the highest posterior probability is taken as the class of x . The posterior probability can be calculated into the following equation, according to the Bayes formula:

$$p(|Y = c_k|X = x) = \frac{p(|X = x|Y = c_k)p(Y = c_k)}{\sum_k p(|X = x|Y = c_k)p(Y = c_k)}, \quad (9)$$

where, X is the input feature set, $x \in X$; Y is the category set, $Y \in \{c_1, c_2, \dots, c_k\}$, $k = 1, 2, c_1 = 1$ indicates normal driving condition, $c_2 = -1$ is the fatigue driving state. Formula (10) can be obtained by expanding formula (9) with the full probability formula.

$$p(|Y = c_k|X = x) = \frac{p(Y = c_k) \prod_j p(X^{(j)} = x^{(j)}|Y = c_k)}{\sum_k p(Y = c_k) \prod_j p(X^{(j)} = x^{(j)}|Y = c_k)}. \quad (10)$$

According to equation (10), the naive Bayes classifier is established in the following equation:

$$y = f(x) = \arg \max_{c_k} \frac{p(Y = c_k) \prod_j p(X^{(j)} = x^{(j)} | Y = c_k)}{\sum_k p(Y = c_k) \prod_j p(X^{(j)} = x^{(j)} | Y = c_k)}. \quad (11)$$

Since the denominator in equation (11) is the same for all CK, the classifier can be further simplified into the following equation:

$$y = f(x) = \arg \max_{c_k} P(Y = c_k) \prod_j p(X^{(j)} = x^{(j)} | Y = c_k). \quad (12)$$

The advantage of the naive Bayes classifier is that the logic of the algorithm is relatively simple and easy to implement. The time and space cost of algorithm implementation is small. It has a stable performance [21], and has little difference in the classification effect for data sets with different data characteristics, that is, the model has good robustness. Naive Bayes classification is not to absolutely assign a sample to a class, but to calculate the posterior probability of the sample belonging to each class, and then map the sample to the class with the maximum posterior probability. And generally, all attributes are in the naive Bayes classifier. In the classification process, all attributes play a direct or indirect role, that is, all attributes participate in the classification, instead of simply deciding the result by one or a few attributes. Although the independence of class conditions between attributes is difficult to be satisfied in practice, it still has a good classification performance, mainly for the following reasons: a relatively few parameter estimates ensure the stability of the estimates. Although the estimated probabilities are biased, the classification principle is based on the order of posterior probabilities, so even if there is a slight deviation in the classification process, it does not matter. In general, data preprocessing is carried out in the early stage of modeling, during which highly correlated variables may be screened, etc., which also improves the data quality for classification to a certain extent.

A naive Bayes classifier also has some defects, and it is difficult to satisfy the hypothesis of class condition independence between attributes in practical application. If the conditional attributes in the data set are highly correlated, it is difficult to achieve the expected classification effect by using the naive Bayes classifier directly. On the other hand, when the data set is incomplete or there is extremely unbalanced data, the deviation of the posterior probability of individual attributes may be large, and the final classification result may be inaccurate. In addition, the quasi-prior probability and quasi-conditional probability needed to be calculated in the classification process of this model are estimated by using the training set, and then the class label of unknown samples is specified according to the formula. Therefore, the noise

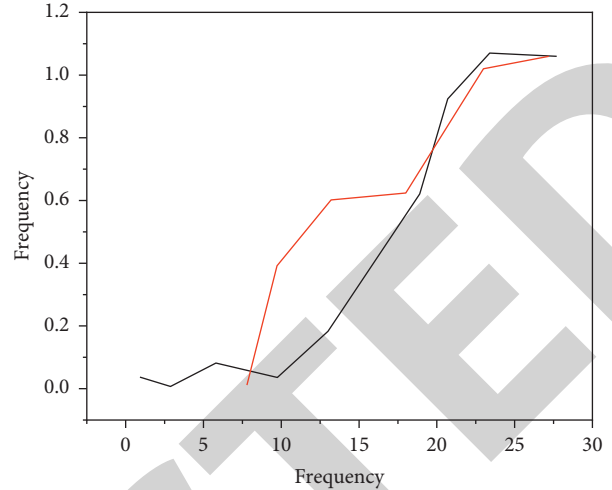


FIGURE 5: Sample frequency values.

in the data set will also have a certain influence on the classification result.

4. Results Analysis

In order to verify the feasibility of the algorithm, several videos of drivers' normal driving and fatigue driving were collected to verify the algorithm.

Blink frequency, yawn frequency, nod frequency, and other characteristic values in the video of driver fatigue and normal state were counted in the experiment. Firstly, a sample in the driving process was used to illustrate the selection process of positive and negative samples in classifier training, as shown in Figure 5. In the part shown, the driver is in the normal driving state, in which the yawn and nod frequency is 0, and the blink frequency is between 0 and 0.06. At this time, the driver is focused and has a good sense of control of the vehicle. In the part, when the driver appeared mild fatigue, he began to yawn and blink frequently. The yawning frequency and blink frequency increased, and the driver appeared distraction phenomenon at this time. With the further deepening of the fatigue degree, in some parts, the driver began to nod, eyes closed for a long time, and other phenomena, at this time, the driver has entered the severe fatigue state, completely lost the consciousness of controlling the vehicle.

Therefore, according to the value changes of blink frequency, yawn frequency, and nod frequency in the normal state and the fatigue state of the driver [22], corresponding positive and negative samples can be made for training and testing of the naive Bayes classifier. During the experiment, a total of 1520 samples were selected, of which 740 were positive samples (normal driving); 780 negative samples (fatigue driving) [23]. In the training and testing of the naive Bayes classifier, there are 910 training samples, 610 test samples, 30 misclassification numbers, and the classifier accuracy rate is 95.08%, as shown in Table 1 [24].

TABLE 1: Naive Bayes classifier test.

| The total number of samples | Number of training samples | Number of test samples | Number of samples incorrectly checked | Accuracy rate (%) |
|-----------------------------|----------------------------|------------------------|---------------------------------------|-------------------|
| 1520 | 910 | 610 | 30 | 95.08 |

TABLE 2: Actual driving environment test.

| Test parameters | Test video 1 | Test video 2 |
|----------------------|--------------|--------------|
| Total video frames | 685 | 714 |
| Eyes closing frames | 407 | 72 |
| Yawn frames | 80 | 104 |
| Nod frames | 124 | 72 |
| Testing number | 19 | 20 |
| Number of mistakes | 1 | 1 |
| Accuracy rate (%) | 94.74 | 95.00 |
| Average accuracy (%) | 94.87 | |

In order to further verify the performance of the naive Bayesian classifier in actual driving, two sample videos were selected for testing in the driver's operating environment, and the test results are shown in Table 2. In video sample 1, a total of 19 times of driver fatigue were detected, including 1 misjudgment with an accuracy of 94.74%; in video sample 2, a total of 20 times of driver fatigue were detected, including 1 misjudgment with an accuracy of 95.00% [25].

5. Conclusion

- (1) The supervised descent algorithm model is used to locate multiple facial features of drivers, and on the basis of which multiple eigenvalues reflecting the driver fatigue state are extracted to establish the corresponding positive and negative sample data.
- (2) The naive Bayes classifier is trained to be used to warn drivers whether they are driving fatigue or not, and the average accuracy is 94.87% in the actual driving test.
- (3) The algorithm only discriminates the fatigue state based on facial features, and more factors, such as driver attention, physiological state, weather, and vehicle driving condition, should be further considered in the subsequent work.

Data Availability

The data used to support the findings of this study are available from the corresponding author upon request.

Conflicts of Interest

The authors declare that they have no conflicts of interest.

Acknowledgments

The project was supported by the Natural Science Foundation of Hunan China (Grant no. 2021JJ60038).

References

- [1] Q. Zhuang, Z. Kehua, J. Wang, and Q. Chen, "Driver fatigue detection method based on eye states with pupil and iris segmentation," *IEEE Access*, vol. 8, Article ID 173440, 2020.
- [2] W. Wang, H. Li, D. Kong, M. Xiao, and P. Zhang, "A novel fatigue detection method for rehabilitation training of upper limb exoskeleton robot using multi-information fusion," *International Journal of Advanced Robotic Systems*, vol. 17, no. 6, Article ID 172988142097429, 2020.
- [3] F. Zhang and F. Wang, "Exercise fatigue detection algorithm based on video image information extraction," *IEEE Access*, vol. 8, Article ID 199696, 2020.
- [4] A. Nemcova, V. Svozilova, K. Bucshazy et al., "Multimodal features for detection of driver stress and fatigue: review," *IEEE Transactions on Intelligent Transportation Systems*, vol. 22, no. 6, pp. 3214–3233, 2021.
- [5] B. Bakker, B. Zablocki, A. Baker et al., "A multi-stage, multi-feature machine learning approach to detect driver sleepiness in naturalistic road driving conditions," *IEEE Transactions on Intelligent Transportation Systems*, vol. 23, no. 5, pp. 4791–4800, 2022.
- [6] E. M. Nowara, T. K. Marks, H. Mansour, and A. Veeraraghavan, "Near-infrared imaging photoplethysmography during driving," *IEEE Transactions on Intelligent Transportation Systems*, pp. 1–12, 2020.
- [7] C. M. T. Gonzalez, J. B. A. Hernandez, J. M. C. Rodriguez, S. T. P. Suarez, D. D. L. C. S. Rodriguez, and A. G. R. Garcia, "Robust detection of fatigue parameters based on infrared information," *IEEE Access*, vol. 9, pp. 18209–18221, 2021.
- [8] C. Ding, W. Tian, C. Geng, X. Zhu, Q. Peng, and Z. Zhao, "Multi-template supervised descent method for face alignment," *Cognitive Systems Research*, vol. 65, no. 12, pp. 107–117, 2021.
- [9] R. Guo, M. Li, F. Yang, S. Xu, and A. Abubakar, "Application of supervised descent method for 2-d magnetotelluric data inversion," *Geophysics*, vol. 85, no. 4, pp. WA53–WA65, 2020.
- [10] H. Lu and R. Mazumder, "Randomized gradient boosting machine," *SIAM Journal on Optimization*, vol. 30, no. 4, pp. 2780–2808, 2020.
- [11] R. Akrou, A. Atamna, and J. Peters, "Convex optimization with an interpolation-based projection and its application to deep learning," *Machine Learning*, vol. 110, no. 8, pp. 2267–2289, 2021.
- [12] A. Albanna and H. Yousefi Zadeh, "Congestion minimization of LTE networks: a deep learning approach," *IEEE/ACM Transactions on Networking*, vol. 28, no. 1, pp. 347–359, 2020.
- [13] M. Kowsher, I. Hossen, A. Tahabilder et al., "Sdsv: angle measurement for supervised classification," *Procedia Computer Science*, vol. 189, pp. 216–223, 2021.
- [14] Z. Fu, Y. Zhao, Y. Xu, L. Xu, and J. Xu, "Gradient structural similarity based gradient filtering for multi-modal image fusion," *Information Fusion*, vol. 53, pp. 251–268, 2020.
- [15] D. Gomez and J. Wei, "Multi-spike patterns in the Gierer–Meinhardt system with a nonzero activator boundary flux," *Journal of Nonlinear Science*, vol. 31, no. 2, p. 37, 2021.

- [16] S. Wang, Y. Guan, and L. Shao, "Multi-granularity canonical appearance pooling for remote sensing scene classification," *IEEE Transactions on Image Processing*, vol. 29, pp. 5396–5407, 2020.
- [17] J. Yang, Y. Huang, R. Zhang, F. Huang, Q. Meng, and S. Feng, "Study on ppg biometric recognition based on multifeature extraction and naive Bayes classifier," *Scientific Programming*, vol. 2021, no. 12, pp. 1–12, 2021.
- [18] V. Jackins, S. Vimal, M. Kaliappan, and M. Y. Lee, "Ai-based smart prediction of clinical disease using random forest classifier and naive Bayes," *The Journal of Supercomputing*, vol. 77, no. 5, pp. 5198–5219, 2020.
- [19] Y. Zhang and A. Jatowt, "Estimating a one-class naive Bayes text classifier," *Intelligent Data Analysis*, vol. 24, no. 3, pp. 567–579, 2020.
- [20] A. K. Gupta and N. Sardana, "Performance analysis of naive Bayes classifier over similarity score-based techniques for missing link prediction in ego networks," *Journal of Information Technology Research*, vol. 14, no. 1, pp. 110–122, 2021.
- [21] G. Li, F. Liu, A. Sharma et al., "Research on the natural language recognition method based on cluster analysis using neural network," *Mathematical Problems in Engineering*, vol. 2021, Article ID 9982305, 13 pages, 2021.
- [22] J. Jayakumar, B. Nagaraj, P. Ajay, and P. Ajay, "Conceptual implementation of artificial intelligent based E-mobility controller in smart city environment," *Wireless Communications and Mobile Computing*, vol. 2021, Article ID 5325116, 8 pages, 2021.
- [23] X. Liu, J. Liu, J. Chen, F. Zhong, and C. Ma, "Study on treatment of printing and dyeing waste gas in the atmosphere with Ce-Mn/GF catalyst," *Arabian Journal of Geosciences*, vol. 14, no. 8, p. 737, 2021.
- [24] R. Huang, P. Yan, and X. Yang, "Knowledge map visualization of technology hotspots and development trends in China's textile manufacturing industry," *IET Collaborative Intelligent Manufacturing*, vol. 3, no. 3, pp. 243–251, 2021.
- [25] Q. Zhang, "Relay vibration protection simulation experimental platform based on signal reconstruction of MATLAB software," *Nonlinear Engineering*, vol. 10, no. 1, pp. 461–468, 2021.